Dielectric Characterization

Aly Franck, TA Instruments, New Castle DE, USA

ABSTRACT

The Dielectric measurement module for dynamic mechanical instruments or rheometers can be used as standalone device, taking advantage of the instrument temperature control system and can be operated in conjunction with the mechanical instrument to provide a simultaneous dielectric-mechanical characterization on the same sample. This product note includes theoretical beackground information on dielectric measurements and details on how the dielectric module is integrated and operated with TA Instruments dynamic mechanical instruments. Two application examples (polymers and emulsions) provide inside into the wide application of standalone dielectric and simultaneous dielectric -mechanical measurements.

CONTENTS:

1. INTRODUCTION

Dielectric analysis is the study of the mobility of dipoles or ions in a material. The mobility of these charged groups is measured by applying an oscillatory voltage to the sample and by recor-ding the current.

The measured impedance is related to two dielectric properties; the capacitance or the capability to store charges in the material and the conductance or mobility of charged carrier in the material.

Physical and chemical structure properties as well as process behaviour of many materials can be investigated through the measurement of their dielectric properties. Dipoles in a material will attempt to orient with the applied electrical field while ions will migrate towards the electrodes of opposite polarity.

Changes in the degree of alignment of dipoles as a function of temperature and frequency provide information about physical transitions; changes in the mobility of ions correlate to the material viscosity and reaction kinetics of evolving systems

2. THEORETICAL BACKGROUND

Dielectric measurements

In an dielectric measurement a voltage is applied across two electrodes in contact with the material to determine its capaci-

tance. A material is classified as 'dielectric' if it has the ability to store energy when an external field is applied. A dielectric material increases the storage capability by neutralizing charges at the electrode. The highest charge is stored in the capacitor when the material between the plates has a high dielectric constant. The capacitance is defined as:

$$C = C_o \kappa'$$ (1)

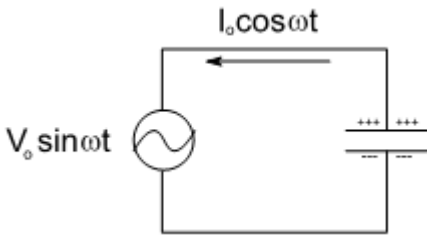κ' is the dielectric constant, C_o is the capacitance in free space (vacuum).

Figure 1: A current $I_c(t)=I_o cos\omega t$ charges the capacitor when a sinusoidal voltage $V(t)=V_o sin\omega t$ is applied

When a sinusoidal voltage $V(t)=V_o sin\omega t$ is applied to a capacitor, a current $I_c(t)$ is drawn to charge the capacitor plates (Figure 1). The charge at the electrode plates is $Q=C_o V$ when the medium between the plates is free space. The current is the time derivative of the charge.

$$I_c(t) = \frac{dQ}{dt} = I_o cos\omega t$$ (2)

In addition to the charging current, a loss current component may also be present. This is the leaking current dissipated by the electrical resistance R in the material according to:

$$I_l(t) = \frac{V}{R} = GV$$ (3)

G is the conductance.

The total current drawn is the sum of the current related to the stored charges and the losses in the material when represented by a resistance in parallel with a capacity as shown in figure 2.
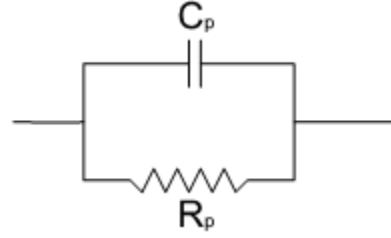
$$I(t) = I_c + I_l$$ (4)

Figure 2: Equivalent parallel circuit with resistance and capacity in parallel

With $V=V_o e^{i\omega t}$ and the charge current $Q=CV$, (2) can be rewritten as:

$$I_c = \frac{dQ}{dt} = \frac{dCV}{dt} = \frac{d}{dt}(CV_o e^{i\omega t})$$

$$= i\omega CV_o e^{i\omega t} = i\omega CV$$ (5)

With (3) and (5) the total current can be evaluated as:

$$I = I_c + I_l = V(i\omega C + G)$$ (6)

Inserting (1) into (5) gives:

$$I = V(i\omega C_o \kappa' + G)$$

Integrating the loss current contributions into the dielectric constant provides:

$$I = V(i\omega C_o \kappa' + \omega C_o'')$$

$$= V(i\omega C_o)(\kappa' - i\kappa'')$$ (7)

$C_o''/C_o = \kappa''$ is the dielectric conductance and $\kappa^* = \kappa' - i\kappa''$ the complex dielectric constant.

The frequency response of this circuit can be expressed in terms of the ratio of charge and loss current (figure 3):
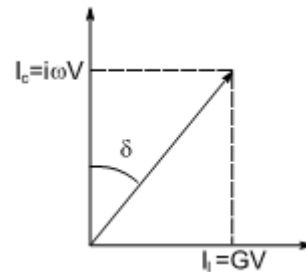

Figure 3: I_c is out of phase and I_l is in phase with the applied voltage

$$\frac{I_c}{I_l} = tan\theta \Rightarrow \frac{I_l}{I_c} = tan\delta = D = \frac{1}{Q}$$ (8)

D is the dissipation factor, Q is referred to as quality factor. Note that the loss current is in phase and the charge current is out of phase with the applied voltage (figure 3).

In a parallel plate capacitor with surface area A and plate separation d, neglecting fringing effects at the border, the capacitance for free space is defined as:

$$C_o = \frac{A}{d}\varepsilon_o \quad and \quad C = \frac{A}{d}\varepsilon \tag{9}$$

ε_o and ε are the permittivity for vacuum respectively the dielectric material. The relative permittivity is defined as:

$$\frac{\varepsilon}{\varepsilon_o} = \varepsilon_r = \frac{C}{C_o} \Rightarrow C = C_o\varepsilon_r \tag{10}$$

Comparison with (1) provides:

$$C = C_o\kappa' = C_o\varepsilon_r' = C_o\frac{\varepsilon'}{\varepsilon_o} \tag{11}$$

Note that the relative storage permittivity is equivalent to the dielectric constant.

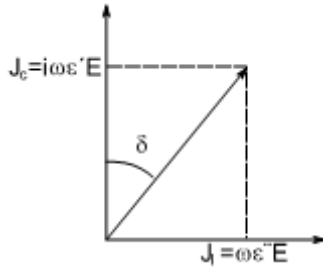The current density J, equal to the total current I per surface area A can be for-

Figure 4: Inphase and Out of phase component of the current density

mulated using (9), (7) and the field strength $E=V/d$ (figure 4) as follows:

$$J = \frac{I}{A} = V(i\omega\varepsilon_r' + \omega\varepsilon_r'')\frac{\varepsilon_o}{d}$$
$$= (i\omega\varepsilon' + \omega\varepsilon'')E$$
$$= \varepsilon^*\frac{dE}{dt} = J_l - iJ_c \tag{12}$$

Data interpretation and models

A dielectric material increases the storage capacity of a capacitor by neutralizing charges at the electrode surface which otherwise would have contributed to the external field (figure 5). Only the free charges contribute to the voltage according to:

$$\frac{Q}{\kappa'} = C_oV \tag{13}$$

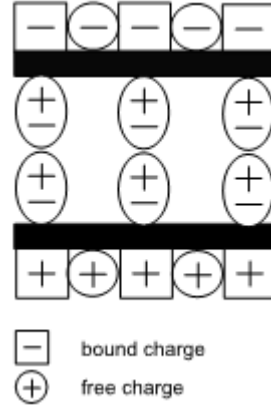
| $-$ | bound charge |
| $+$ | free charge |

Figure 5: Bound and free charges at the electrode surface

The bound charges $Q(1-1/\kappa')$ are neutralized by the dielectric medium. These bound charges give rise to the sample polarization.

The ratio of bound and free charge density is referred to as electric susceptibility of a dielectric material.

Two electric charges of opposite polarity +/-Q separated by a distance d represent a dipole of moment $\mu=Qd$. μ is a vector pointing from the negative to the positive pole. In materials, dipoles manifest themselves by charge asymmetries that exist in molecules or molecule fragments.

If an electric charge is placed in an electrostatic field it is subjected to a force. Accordingly if an external electric field is applied to a material, the dipole fragments will align themselves and partially cancel the effects of the electric field as shown in figure 5. The time that it takes for the

dipole to align varies and depends on the physical properties of the material and the external conditions such as temperature and pressure. Steric hindrance prevents dipoles from fully reorientating in response to the electric field.

This is especially true for solid (semi-crystalline and amorphous polymers) where the polymer chains are rigid so that the dipoles can only reorient slightly, which results in a lower dielectric constant and loss factor. Polymers in a rubbery or viscous flow state have higher dipole mobility and therefore higher dielectric constants i.e. loss factor.

Note that the applied electrical field can also induce dipoles in polymers that do not have intrinsic permanent dipole moments. The ability to 'polarize' the molecular structure depends on the chemical properties of the material and the environment.

When mobile charged carriers such as ions or free electrons are present in a material, they are attracted by the negative i.e. positive electrode. When they overcome the Brownian motion, they drift towards the electrodes - this is referred to as conduction. As the charged species travel through the material, they are slowed down by the surroundings, the slower the ions travel, the higher the resistance. Often the dielectric response consists of both dipole reorientation and conduction, the effects overlap and cannot be distinguished from each other.

A primary goal of dielectric spectroscopy is to characterize relaxation phenomena in materials. Similar to the mechanical spectroscopy, the reorientation of dipoles can be associated with transitions in polymer materials such as the glass transition. The simplest model to descibe the frequency dependence of the permittivity is the Debye model, which is based on a 'hindred reorientation' of dipoles for a single relaxation mechanism.

The relative permittivity can be expressed for a single relaxation time t:

$$\varepsilon_r = \varepsilon_\infty + \frac{\varepsilon_0 - \varepsilon_\infty}{1 + i\omega\tau} \qquad (14)$$

ε_∞ and ε_0 are the permittivities in the 'unrelaxed' and 'releaxed' state. Since dipole orientation and conduction mechanisms can contribute to the dielectric response, a conduction term is often incorporated into the Debye model. Including the conduction term and splitting in real and imaginary components gives the following expresions for the relative permittivity:

$$\varepsilon'_r = \varepsilon_\infty + \frac{\varepsilon_0 - \varepsilon_\infty}{1 + (\omega\tau)^2} \qquad (15)$$

$$\varepsilon''_r = \frac{\sigma}{\omega\varepsilon_0} + \frac{(\varepsilon_0 - \varepsilon_\infty)\omega\tau}{1 + (\omega\tau)^2} \qquad (16)$$

These functions are plotted in figure 6. The conductivity term is responsible for the low frequency tail in the dielectric loss. ε_0 corresponds to the relative permittivity when all dipoles have reached maximum reorientation and ε_∞ is the permittivity when the frequency is so high, that the dipoles are
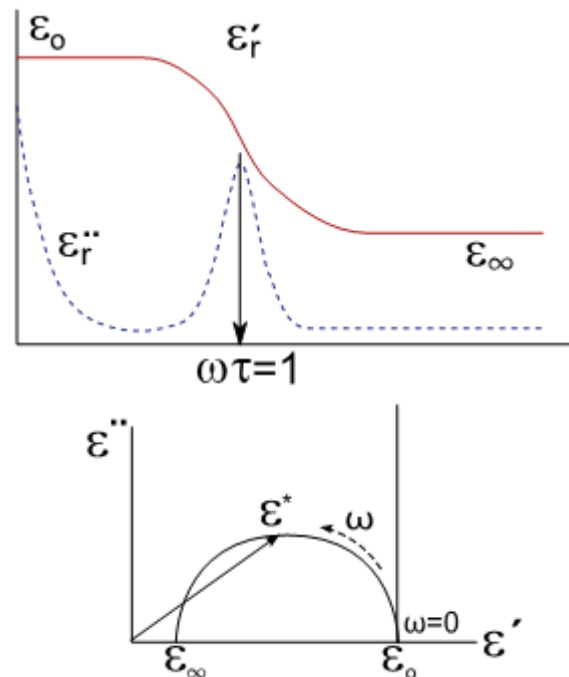

Figure 6: Debye model: Permittivity and loss factor. Cole-Cole plot with ion conduction term ('tail' in complex permittivity)

unable to keep up with the external field. Note that the conductivity term adds the straight line in the Cole-Cole plot when $\varepsilon' = \varepsilon_o$. The maximum loss factor, associated with energy absorption or dampoing by the material, is indicated by the peak at $\omega = 1/t$.

The Debye model with one single relaxation time is qualitative at best. Most relaxation phenomena in materials are represented by more than one relaxation time. A generalization of the Debye model has been proposed by Cole and Cole. Ignoring the conductivity term, they added an empirical fitting factor, α in (14) such that:

$$\varepsilon_r = \varepsilon_\infty + \frac{\varepsilon_o - \varepsilon_\infty}{1 + (i\omega\tau)^{1-\alpha}} \tag{17}$$

Whereas the Debye model shows a perfect semicircle in figure 6, does the Cole-Cole model allow a compressed semicircle with the center below the ε' axis.

Another empirical modification with two fit parameters has been introduced by Havriliak and Negami to allow both flatness and unsymmetricak skew for the Cole-Cole plot.

$$\varepsilon_r = \varepsilon_\infty + \frac{\varepsilon_o - \varepsilon_\infty}{[1 + (i\omega\tau)^\alpha]^b} \tag{18}$$

3. EXPERIMENTAL

Parallel plate electrode:

In a dielectric measurement, a sample is placed in contact with two electrodes and a time-varying (sinusoidal) voltage is applied across the electrodes. From the measured current and the applied voltage an electrical impedance is obtained which is then converted to sample permittivity by incorporating the electrode geometry.

The impedance measurement can be accomplished using a frequency response analyzer or an impedance bridge. The frequency response analyzer measures the voltage and current signal, the impedance bridge (LCR meter) uses an adjustable impedance to balance the impedance of the sample. The later is most commonly used for dielectric instruments in the frequency range from 10^{-3} to 10^7 Hz.

In a plate-plate arrangement, the sample is placed between disc shaped electrodes with an area A and a separation d. Assuming that boundary or fringing effects are negligible and the space between the electrodes is vacuum, the capacitance C_o of the capacitor is :

$$C_o = \frac{A\varepsilon_o}{d} \tag{19}$$

e_O is the permittivity of free space and has a value of 8.8452pF/m.

Note: Instead of parallel plate electrodes, concentric cylinder electrodes can be used. The capacitance C_o in this case has to be calculated as follows:

$$C_o = \frac{2\pi l\varepsilon_o}{\ln\left(b/a\right)} \tag{20}$$

b is the outer electrode radius, a the inner electrode radius and l the electrode length.

Parallel plate electrodes have become common practice to measure a solid or melt sample specimen of flat circular disc shape. Soft solids and liquid samples can be measured in a parallel plate arrangement as well. It is however essential that the area and the thickness is known accurately in order to obtain the correct values for the capacitance and the resistance. Good electrical contact between sample and electrode plates has to be ensured in order to avoid error due to trapped air; an additional capacitance in series with the sample would be introduced. This is less a problem for liquid samples than for solid materials. A metal film can be evaporated on solid disc samples to improve contact and minimize errors.

While performing temperature scans, the density of the material changes and consequently the sample gap. The Axial control

feature of the rheometer can be used to control the sample gap throughout the experiment and correct for gap changes during the measurement.

The flow of the electrical field at the sample edge (see figure 1) is not perpendicular. Stray capacitance is formed at the
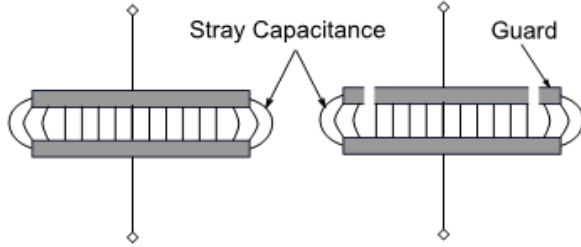

Figure 7: Stray capacitance due to fringe effects. Guard ring design to eliminate fringe effects.

edges of the electrodes causing an increase of the measured capacitance.

A solution is to use a guard electrode. The guard absorbs the electric field at the edge and the capacitance measured between the plate is only composed of the current that flows through the dielectric material.

Equivalent parallel and series circuits

When analyzing the measured impedance it is advantageous to consider the test sample being equivalent to a capacitance C in parallel with a resistance. C and and R are frequency dependent.

For the equivalent circuit of capacitance and resistance in parallel, the electrical
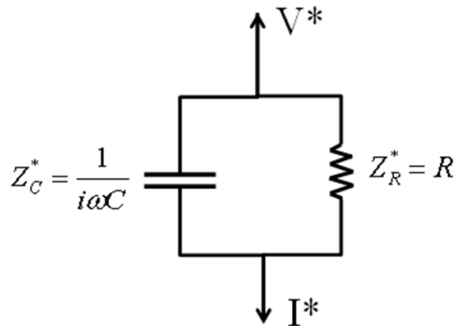

Figure 8: Parallel R-C circuit

admittance (inverse of the impedance) is given by (see figure 8):

$$Y^* = \frac{I^*}{V^*} = \frac{1}{Z^*}$$

$$= \frac{1}{Z_r^*} + \frac{1}{Z_c^*} = \frac{1}{R_p} + i\omega C_p \qquad (21)$$

Rearranging in terms of the impedance $Z^*=Z'+iZ''$ and extracting the real and imaginary components provides:

$$Z' = \frac{R_p}{1 + \omega^2 R_p^2 C_p^2} \qquad (22)$$

$$Z'' = \frac{\omega R_p^2 C_p}{1 + \omega^2 R_p^2 C_p^2} \qquad (23)$$

The dissipation factor D is the ratio of the imaginary and real part of the admittance:

$$D = \frac{Im(Y^*)}{Re(Y^*)} = \frac{1}{R_p C_p \omega} \qquad (24)$$

Note that combining the equations (22) and (23) yields the equation for a circle with radius $R_p/2$

$$\left(Z' - \frac{R_p}{2}\right)^2 + \left(Z''\right)^2 = \frac{R_p^2}{4} \qquad (25)$$

The circle is centered at $Z'=R_p/2$ and $Z''=0$. The representation of Z'' as a function of Z' is referred as Cole-Cole plot. Replacing the complex current with $I^*=[i\omega \varepsilon'+\omega\varepsilon'']C_oV^*$ in equation (21) gives for the real and imaginary components of the complex permittivity ε^* after rearrangement:

$$\varepsilon' = \frac{C_p}{C_o} \qquad \varepsilon'' = \frac{1}{R_p C_o \omega} \qquad (26)$$

Inserting $C_o=A\varepsilon_o/d$ provides the equations used to calculate the experimental results:

$$\varepsilon' = \frac{d C_p}{A\varepsilon_o} \qquad \varepsilon'' = \frac{d}{R_p A\varepsilon_o \omega} = \frac{d G_p}{A\varepsilon_o \omega}$$

$$\tan\delta_\varepsilon = \frac{\varepsilon''}{\varepsilon'} = \frac{1}{\omega R_p C_p} \qquad (27)$$

$G_p = 1/R_p$ is the conductance of the equivalent parallel circuit. R_p and C_p are obtained from the impedance bridge (LCR meter).

When the impedance $Z^* < 100K\Omega$, a serial equivalent circuit is preferred as it allows a more accurate determination of the capacitance. The impedance of the equivalent serial circuit (see figure 9) is:

$$Z^* = Z_c^* + Z_R^* = R_s + \frac{1}{i\omega C_s} \qquad (28)$$

With

$$I^* = [i\omega\varepsilon' + \omega\varepsilon'']C_o V^* = \frac{V^*}{Z^*} \qquad (29)$$

following expressions for the permittivity can be obtained:

$$\varepsilon' = \frac{C_s}{C_o(1 + \tan^2\delta)}$$

$$\varepsilon'' = \frac{R_s C_s^2 \omega}{C_o(1 + \tan^2\delta)}$$

$$\tan\delta_\varepsilon = R_s C_s \omega \qquad (30)$$

The equivalent parallel and series capacitance are related as follows

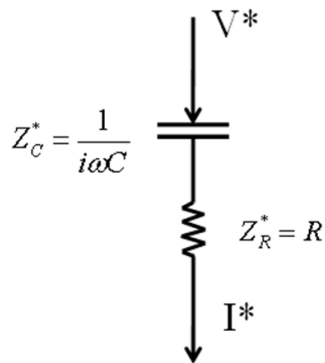Figure 9: Serial R-C circuit

$$C_p = \frac{C_s}{(1 + \tan^2\delta)}$$

$$R_p C_p = \frac{1}{R_s C_s \omega^2} \qquad (31)$$

When $\delta \rightarrow 0$ (conductance $G \rightarrow 0$), the capacitance $C_p = C_s$.

Calibration

The relative permittivity is referenced to the capacitance of free space. However because of fringe effects, the measured capacitance does not only depend on the gap but also of the geometry ratio d/R. Evidently fringe effects decrease with decreasing gap at constant plate radius. For the 25mm plate electrodes included in the dielectic option, the reported permittivity value of air is obtained at a gap of approximately 0.7mm (Figure 10).

In order to compensate for contributions and losses in the connectors and cables, it is also important to calibrate the LCR meter when the electrodes are separated enough to be independent (open) and when they are in contact (short). As such only sample contributiuons are measured.

The TRIOS software does not calculate the relative permittivity. However the dielectric plate setup can be calibrated with air or any other fluid with known relative permittivity as a function of plate separation. When parameterizing this relationship, a calibration factor can be easily calculated using the 'user defined variable' capabilities in TRIOS.

Figure 10 shows the calibration factor defined as ($\varepsilon_{Measured}/\varepsilon_{Reported}$) for the standard 25mm dielectric plate assembly.
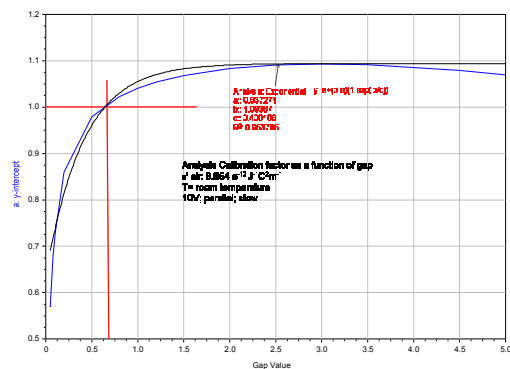

Figure 10: Calibration curve of air as a function of the gap for the standard 25mm dielectric plates with the furnace closed. The measured permittivity of air equals to the reported permittivity of air (8.854 pF/m) at a gap of ~ 0.7mm.

Note that all measurements were performed with the furnace closed. The calibration curve was fittet with an exponential function according to:

$$cf = a + (b - a)\left(1 - e^{\left(-\frac{gap}{c}\right)}\right) \qquad (32)$$

Operation

The dielectric module as part of the rheo-meter system is controlled by the rheometer operation software TRIOS. The software offers three types of operation modes: standalone dielectric measure-ments, combined DMA and dielectric mea-surments and simultaneous single die-lelectric measurements in conjunction with other rheological test modes.

The standalone version does only perform dielectric measurements, however the axial force control of the rheometer is active and provides gap and axial force information. The tests can be run as single frequency sweep, isothermal continuous sweeps, temperature ramps or temperature steps. The dielectric frequency can be changed linear, logarithnmic or discrete.

The combined (hybrid) dielectric/mechani-cal analysis DEA/DMA uses the same test modes as the standalone version, however a dynamic mechanical defor-mation at selected frequency and strain is applied at the same time the dielectric measurement is performed.

The simultaneous single dielectric measurement can be combined with any other test mode. The dielectric measure-ment conditions are set in a conditioning step prior to the mechanical testing mode. The simultaneous dielectric mode can be used to follow changes in a material as a result of the mechanical testing. Note that when combined with transient or flow tests, the total rotation (speed) is limited to avoid breaking the electrode cable connected to the upper or lower test geometry.
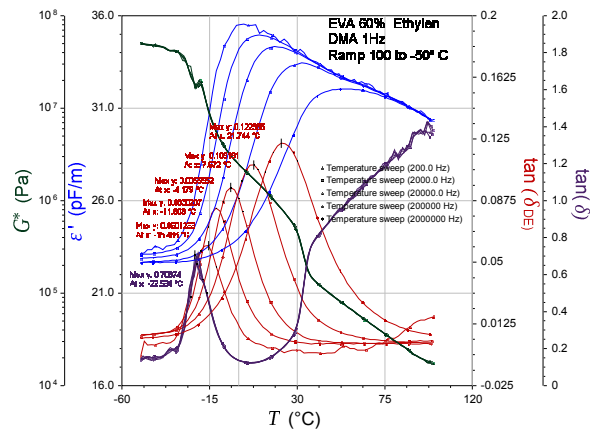

Figure 11: EVA with 60% ethylene. Temperature ramp from 100 to -50 ℃. The dynamic mechanical frequency is 1Hz ; the simultaneous dielectric frequencies are of 200, 2000, 20000, 200000 and 2000000 Hz

Characterizing relaxations in polymers (ethylene vinyl acateate)

3 EVA polymers with an ethylene content of 60, 77 and 82% have been tested using the hybrid DEA/DMA test. This test mode performs a dynamic mechanical test at one oscillation frequency while sweeping a range of dielectric frequencies simultane-ously. Figure 11 shows the combined DMA and DEA response in the temperature range from 100 to -50°C for the ethylene vinyl acetate with an ethylene contenet of 60%.

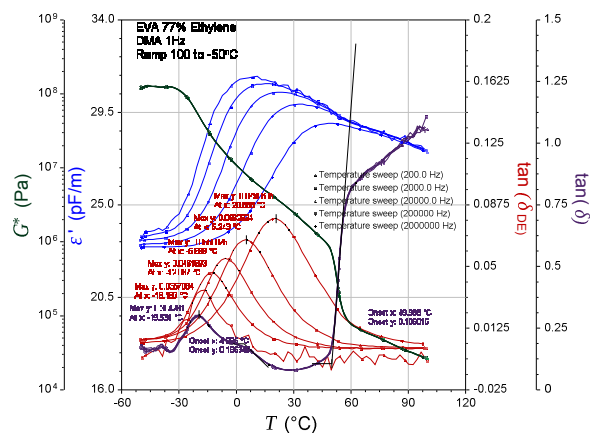The melting point of the crystals in the copolymer exhibit a sharp transition around

Figure 12: EVA with 77% ethylene. Temperature ramp from 100 to -50 ℃. The mechanical frequency is 1Hz and the simultaneous dielectric frequencies
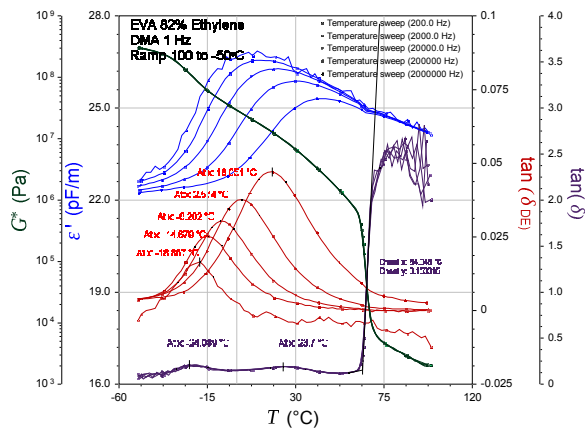
Figure 13: EVA with 82% ethylene. Temperature ramp from 100 to -50 °C. The mechanical frequency is 1Hz and the simultaneous dielectric frequencies are 200, 2000, 20000, 200000 and 2000000 Hz

Ethylen content	60%	77%	82%
2 000 000 Hz	27.7	20.8	18.0
200 000 Hz	7.7	5.3	2.5
20 000 Hz	-4.2	-5.7	-8.2
2 000 Hz	-11.8	-12.8	-14.7
200 Hz	-15.5	-16.8	-18.8
1Hz low transition	-22 (-19)	-19.5	-24
1Hz shoulder	--	4.1	23.7
1Hz onset	29	49.9	64

Table 1: Glass transitions and melting transitions for the 3 EVA copolymers with 60, 77 and 82% ethylene content (Tg of PVAc ~30 °C, of PE~-125 °C).

30°C in the mechanical response, however this transition does not show in the dielectric response. The glass transition appears in the mechanical response around -20°C. This transition is also picked up by the dielectric measurement, the transition temperature increasing with increasing dielectric frequency from -15.5 to 27.7°C.

The melting point for the copolymer with 77% ethylene shifts from 29°C to 49.9°C and the glass transition shows a broad peak in the mechanical response at 19.5°C in figure 12.

In addition, the mechanical loss exhibits a shoulder around 4.1°C which is also not present in the dielectric response. The dielectric transitions are shifted to lower temperature.

For the sample with 82% of ethylene (figure 13), the dielectric transitions are shifted further to lower temperature. The melting point of the crystals shifted up to 64°C. For this composition two small separate glass transitions exist in the mechanical response at -24 and at 23.7°C.

Table 1 summarizes the experimental findings. Mechanical testing is very sensitive to the presence of the crystalline segments of ethylene in the EVA copolymer. The melting point increases with the con-

tent of the semi-crystalline ethylene in the copolymer. This transition is not picked up by the dielectric measurement. The glass transition of the copolymer shows at -22°C for the copolymer with 60% ethylene. At 77% this glass transition becomes broader with a shoulder at 4.1°C. At 82% ethylene content, two separate peaks exist at -24.0°C and 23.7°C. The shoulder and the second peak are probably due to chain rearrangements or relocations in the crystal structure of the polyethylene, which separate out
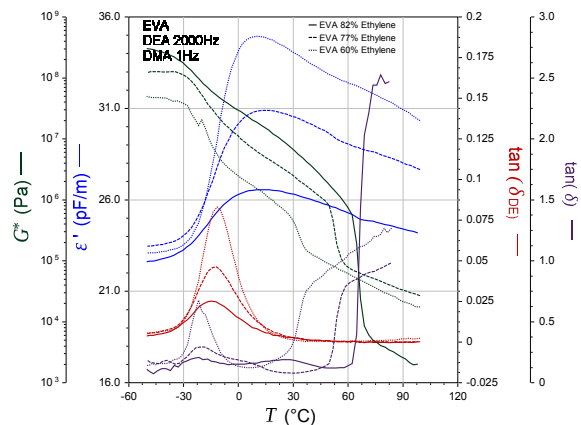

Figure 14 : Temperature ramp of 3 EVA samples with an ethylene content of 60, 77 and 82%. The mechanical (1Hz) and dielectric (2000Hz) response isare shown

from the copolymer glass transition at -24° C as the melting point of the crystal segments increases with increasing ethylene content.

Figure 14 shows an overlay of the mechanical response at 1 Hz and the dielectric response at 2000Hz for the three EVA copolymers. The graph shows a glass transition at ~-20 to -24°C in the mechanical and -10 to -15°C in the dielectric response. The transition temperature is almost insensitive to the ethylene content, the magnitude however decreases significantly with decreasing vinylactate (increasing ethylene) content.

Structure changes during cooling and heating of an emulsion

A commercial hand cream has been subject of a cooling/heating cycle from 30 to -30°C and back to 30°C.

After loading, the emulsion is heated to 30°C before starting the cooling/heating cycle. When cooling down the permittivity is changing very little; the dielectric loss almost at zero. The transition at -13°C is due to the crystallization of the water which also pairs with the break down of the cream (phase separation); the permittivity decreases as the cream cools down further. During the heating cycle, both loss and storage permittivity increase drastically with a transition in the vincinity of 0°C,
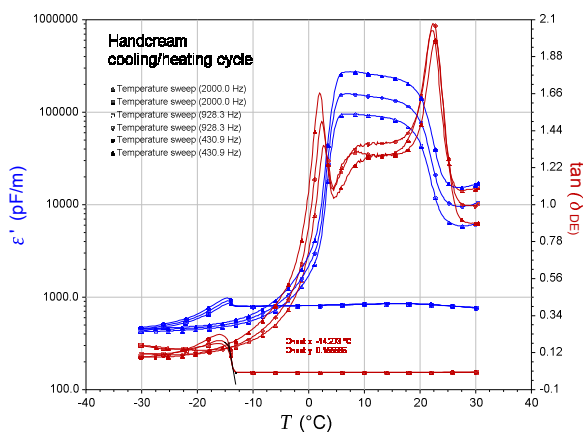

Figure 15: Cooling-heating cycle for a typical handcream

marking the melting of the water which has separated out during the cooling process. This transition shifts to higher temperature and decreases in magnitude with increasing dielectric frequency. The second transition at 25°C is probably the melting of the wax. The extensive increase in the permittivity is due to the free water, saturating the capacitor plates.

5. CONCLUSIONS

Dielectric characterization is a very powerfull tool to evaluate structure parameters and physical changes in a dielectric material. Dielectric measurements conducted simultenously with mechanical measurements can significantly enhance the available information in order to better understand the processes taking place during a mechanical measurement.

A dielectric characterization module, available as an option for a dynamic mechanical instrument or rheometer takes advantage of the parallel plate or concentric cylinder flow cells which are used for mechanical testing as well as the axial force control to determine the separation of the plate electrodes when sample dimenions change during temperature scans.

REFERENCES:
A.Von Hippel; Handbook of Physics by E.U. Condon; H.Odishaw, Chapter 7. Dielectrics; McGrw-Hill,NewYork (1967)

J.W.Schulz; Encyclopedia of Analytical Chemistry by R.A. Meyers, Dielectric Spectroscopy in Analysis of Polymers; John Wiley & Sons Ltd. (2011)

K.S.Cole, R.H.Cole, J.Chem.Phys. 9, 341 (1941) Dispersion and absorption in Dielectrics

F.P. Reding, J.A. Faucher, R.D.Whitman, J.Pol.Sci, 57, 483-498 (1962)